



# Human health risk apportionment from potential sources of heavy metals in agricultural soils and associated uncertainty analysis

Guanghui Guo · Yuntao Wang · Degang Zhang · Kai Li · Mei Lei

Received: 28 April 2021 / Accepted: 25 February 2022 / Published online: 29 March 2022  
© The Author(s), under exclusive licence to Springer Nature B.V. 2022

**Abstract** Evaluating heavy metal pollution level in the soils and apportioning the source-specific health risk of heavy metals are critical for proposing environmental protection and remediation strategies to protect human health. This study explored heavy metal pollution and associated source-specific health risks in a typical rural industrial area, southwestern China. A total of 105 topsoil samples were collected and the concentrations of heavy metals, including As, Cd, Cr, Cu, Ni, Pb and Zn, were determined. Pollution load index and enrichment factors were used to evaluate the pollution level of heavy metals. Positive

matrix factorization (PMF) model was applied to apportion the heavy metals and the associated source-specific health risks to adults and children were estimated via combining the PMF model with the health risk assessment. The results indicated that the soils were highly polluted by multiple heavy metals, especially for Cd, with the EF values of 24.94 and 22.55 in the upstream and downstream areas, respectively. Source apportionment results showed that atmospheric deposition, smelting activities, fertilizer and sewage application, and agrochemical utilization were the main anthropogenic sources, with the contributions of 37.11%, 23.69%, 19.69%, and 19.51%, respectively. Source-specific risk assessment identified atmospheric deposition as the priority source for the non-carcinogenic (NCR) and carcinogenic risks (CR) in the study area, with the contribution of 43.71% and 52.52% for adults, and 44.29% and 52.58% for children, respectively. Moreover, non-carcinogenic and carcinogenic risks posed to children (NCR: 2.84; CR:  $1.31 \times 10^{-4}$ ) from four sources was higher than those posed to adults (NCR: 0.29; CR:  $5.86 \times 10^{-5}$ ). The results of source-specific health risk assessment provided the valuable information on the priority sources for pollution preventing and risk controlling.

**Supplementary Information** The online version contains supplementary material available at <https://doi.org/10.1007/s10653-022-01243-7>.

G. Guo · Y. Wang · D. Zhang · K. Li · M. Lei (✉)  
Institute of Geographic Sciences and Natural Resources  
Research, CAS, Beijing 100101, China  
e-mail: Leim@igsnr.ac.cn

G. Guo  
e-mail: Guogh@igsnr.ac.cn

Y. Wang  
e-mail: Wangyt.16b@igsnr.ac.cn

D. Zhang  
e-mail: Zhangdg.17b@igsnr.ac.cn

K. Li  
e-mail: Lik.18b@igsnr.ac.cn

G. Guo · Y. Wang · D. Zhang · K. Li · M. Lei  
University of Chinese Academy of Sciences,  
Beijing 100049, China

**Keywords** Heavy metals · Agricultural soils · Source apportionment · Source-specific health risk · Priority source

## Abbreviations

HMs	Heavy metals
PMF	Positive matrix factorization
ICP-MS	Inductively coupled plasma mass spectrometer
PI	Pollution index
PLI	Pollution load index
EF	Enrichment factor
THI	Total hazard index
HI	Hazard index
TCR	Total carcinogenic risk
CR	Carcinogenic risk
RfD	References dose
SF	Slope factor
K–S test	Kolmogorov–Smirnov test
BS	Bootstrap
DISP	Displacement
RSV	Risk screening values
Min	Minimum
Max	Maximum
Med	Median
SD	Standard deviation
CV	Coefficients of variation
GM	Geometric mean
BV	Background values
F1, F2, F3, F4	Factor 1, factor 2, factor 3, factor 4

## Introduction

Due to the rapid industrialization and urbanization, heavy metals (HMs) were discharged and accumulated in the agricultural soils. HMs attracted great environmental concern because of their toxicity, persistence, and bioaccumulation (Cortada et al., 2018). Generally, HMs in agricultural soils are controlled by natural background levels and anthropogenic input. Natural sources included parent material and weathering of rocks (Duan et al., 2020; Huang et al., 2018). Anthropogenic activities included nonferrous mining and smelting (Hu et al., 2019), fertilizers and agrochemical application (Wang, et al., 2019), sewage irrigation (Marrugo-Negrete et al., 2017), sludge application (Khadhar et al., 2020), and vehicle exhaust (Khademi et al., 2019). It is essential to characterize the pollution levels of soil HMs, apportion their potential sources, and understand the associated source-specific health risks for environmental management and protection.

In order to effectively prevent the HM pollution of agricultural soils, it is critical to identify the priority sources of HMs. It should be noted that source apportionment of HMs is a challenging task in the area where multiple and complex pollution sources coexist. Positive matrix factorization (PMF) has been used for source apportionment of HMs in agricultural soils (Cai et al., 2019; Jiang et al., 2021), urban soils (Duan et al., 2020) and atmospheric particulates (Zheng et al., 2019). However, the historical sources that contributed to the soil HMs are hard to track as the sources may have disappeared, and thus factors derived from PMF model were usually interpreted based on the common knowledge of the previous studies, leading to the subjectivity of the results of source apportionment. In order to overcome these challenges, the uncertainty of the PMF result was further analyzed based on the Bootstrap (BS) and displacement (DISP) methods. Moreover, geo-statistical analysis was used to depict the spatial intensity of potential sources and interpret the factors derived from PMF model, which is essential to reveal the actual scenario of source apportionment.

In addition, most of current researches only focus on the receptor risk of HMs in soil sampling sites, ignoring the source contribution to the risk. In fact, heavy metal constituents differed from the pollution sources, and the largest source contribution to soil HMs may not pose the highest human health risks (Jiang et al., 2020; Liu et al., 2018). Therefore, source-specific risk apportionment should be analyzed to identify the priority sources based on the comprehensive approach combining the source apportionment with the health risk assessment.

The typical mining and smelting industries based on the smelting and processing of nonferrous metals is located in the Southwestern China. Agricultural production is also well developed in this area, with the high application of fertilizers and pesticides. Overall, this area is highly exposed to various HM sources. Thus, it is critical to investigate the pollution status of HMs in the agricultural soils of this area and quantify the source-specific risk contribution to local people. In our previous study, a source-specific risk apportionment method has been developed at the county level (Guo et al., 2021); however, the practicability of this method in the field scale is not clear.

The objectives of this study were: (1) to characterize the pollution level of HMs in agricultural soils;

(2) to apportion the source contribution to soil HMs using PMF model assisted with GIS-mapping and further analyze the associated uncertainty; and (3) to quantitatively determine the source-specific health risks apportionment combining source apportionment with health risk assessment. The results of this study are beneficial for decision-makers to take cost-effective pollution prevention strategies.

**Material and methods**

**Study area**

The study area, a typical rural industrial area in northeast Yunnan Province, China, is characterized by a complex of industrial and agricultural activities (Fig. 1). It has a population of 81,000. The river flows from southwest to northeast in the study area. This area is surrounded by roads, villages, and various industrial plants. There are national highways and township roads through the study area. The major industries near the study area include a large Zn smelting, metal casting plants, building material processing, machine manufacturing, and cement plants. Particularly, Zn smelting plants have developed rapidly and contributed greatly to local economic development. According to the yearbook (LPG, 2019), production of Pb, Zn, and Cd in 2019 was approximately 3659, 4088, and 369 t, respectively. Moreover,

this area has also been associated with traditional agricultural activities, largely focused on the production of rice, rapeseed, and corn. In some locations, vegetables were planted for self-sufficiency. Overall, intensive industrial activities, agricultural activities, and transportation contributed to the accumulation of HMs in the soils.

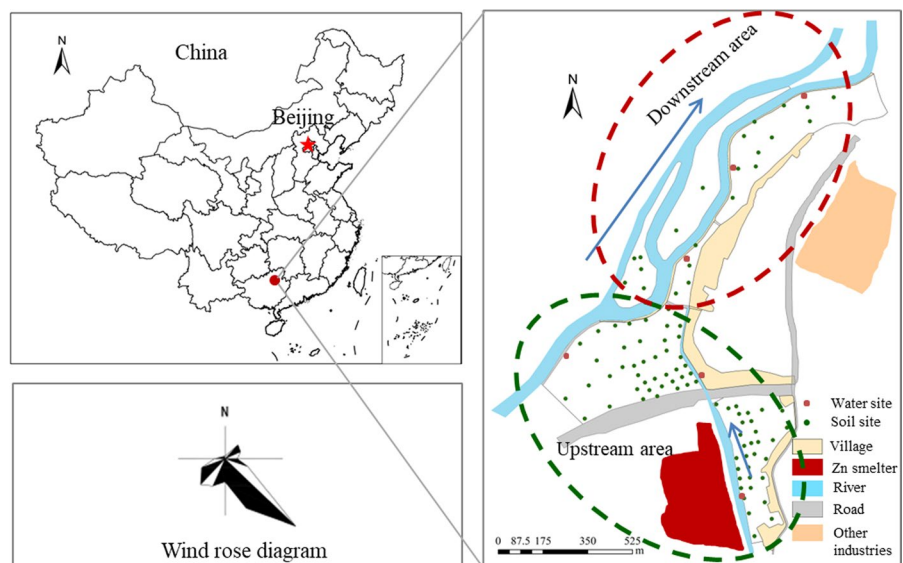
This study area has a typical plateau monsoon climate, with an average annual temperature of 15.1 °C and average annual rainfall of 1700 mm. The prevailing wind direction was mostly southeast, and the annual average wind speed was 3.6 m/s. The predominant soil type in the study area was yellow soil based on the classification and codes for Chinese soil (GB/T17296-2009) (SAPRC, 2009).

**Sampling and preparation**

*Soil samples*

In August 15–20, 2019, a total of 105 topsoil samples (0–20 cm) were collected from agricultural soils, and the sampling locations are shown in Fig. 1. The topsoil sampling site was recorded according to a grid-point sampling strategy. Five sub-samples were randomly collected within a radius of 4 m from the central sampling point (within about 50 m<sup>2</sup>), and then the sub-samples were mixed to obtain a composite sample, which was used as the sample at the central sampling point (MEEC, 2014). Soil samples were

**Fig. 1** The sampling location and study area



collected using a stainless-steel shovel and stored in polyethylene bags, and transported to the laboratory. All soil samples were air-dried at room temperature (20–25 °C) for one week and sieved through a 2-mm mesh to remove plant roots, animal debris, and gravel. Representative portions of each soil sample were ground further with an agate mortar and sieved through a 0.149 mm polyethylene sieve.

Approximately 0.1 g of each homogenized soil sample was weighed and digested with HNO<sub>3</sub>-H<sub>2</sub>O<sub>2</sub> (10:5) using electric hot plates according to the method 3050B (USEPA, 1996). Briefly, the solutions were digested to transparency liquid on the electric hot plates at the temperature of 120 °C, and then cooled at the room temperature. The digestion solutions were then diluted to a volume of 50 mL with deionized water for instrumental analysis.

#### *Irrigation water samples*

Six irrigation water samples were randomly collected from the irrigation canals according to the HJ/T91-2002 (MEPRC, 2002) at the same time (Fig. 1). About 500 mL water samples were transferred to the polyethylene bottles with HNO<sub>3</sub> (0.1%, v/v) to reduce the biodegradation, and then stored at -20 °C until the samples were analyzed.

#### *Chemical analysis*

The concentrations of Arsenic (As) were determined using atomic fluorescence spectrometry (HG-AF8900; Beijing Haiguang Instrumental Co., Ltd., Beijing, China), whereas the concentrations of Cadmium (Cd), Chromium (Cr), Copper (Cu), Iron (Fe), Nickel (Ni), Lead (Pb), and Zinc (Zn) in the digest solution were determined with inductively coupled plasma mass spectrometer (ICP-MS ELAN DRC-e, PerkinElmer, the USA). The standard curves were constructed from the analysis of a multi-element calibrations standard material (PE N9300233, PerkinElmer, Waltham, Massachusetts, USA). The limit of detection (LOD) and limit of quantification (LOQ) were defined as 3 and 10 times of the standard deviation of blank measurements, respectively. The LOD of As, Cd, Cr, Cu, Fe, Ni, Pb, and Zn were 0.12, 0.05, 0.11, 0.08, 0.90, 0.06, 0.09, and 0.67 µg/L, respectively. The LOQ of As, Cd, Cr, Cu, Fe, Ni, Pb, and

Zn were 0.48, 0.2, 0.40, 0.30, 3.0, 0.24, 0.36, and 2.25 µg/L, respectively.

#### *Quality assurance and quality control*

All the glassware and plastic containers were soaked overnight with 20% HNO<sub>3</sub> and rinsed thoroughly with Milli-Q water before use. Chemicals used in this study were guaranteed reagents in the experiments. Moreover, a certified reference soil material (GSS-5/GBW07405, National Research Center for Standards, Beijing, China), procedural blanks, and reagent blanks were included during the sample analysis for quality assurance and control procedures. Replicate samples were also analyzed for 20% of the soil samples and the relative deviation of the duplicated samples was <5%. The recovery rates for As, Cd, Cr, Cu, Fe, Ni, Pb, and Zn in the standard reference materials were 96%–101%, 99%–102%, 99%–105%, 98%–103%, 94%–102%, 95%–99%, 97%–105%, and 94%–106%, respectively.

#### *Pollution assessment*

Pollution index (PI), pollution load index (PLI), and enrichment factor (EF) were used to assess the soil HM pollution level. The calculation equations were described in the supplementary material S1.

#### *Source-specific risk assessment*

A comprehensive approach combining the PMF model with health risk assessment was applied to quantitatively estimate the contribution of health risk from various pollution sources. The procedure of this approach included three steps and then is described as follows:

##### *Step 1: Source apportionment*

PMF is a typical receptor factor approach for source apportionment, which can resolve factor profiles and factor contributions (USEPA, 2014). PMF 5.0 model recommended by United Environmental Protection Agency was applied to apportion the source of soil HMs in this study (USEPA, 2014). The detail information about PMF and uncertainty analysis is described in the supplementary material S2. The model performance parameters are given in Table S1.

*Step 2: Exposure assessment*

The exposure concentrations via incidental soil ingestion, dermal contact, and inhalation from potential sources were estimated based on the results of the source apportionment (USEPA, 1989, 2011). The calculation equations are described in the supplementary material S3. The details of parameters applied in the exposure assessment are given in Table S2.

*Step 3: Source-specific risk characterization*

The non-carcinogenic risks (NCR) for adults and children from potential sources were characterized by total hazard index (THI) of multiple HMs and hazard index (HI) values of individual HMs. The total carcinogenic risk (TCR) is the sum of the carcinogenic risk (CR) of individual HMs from potential sources (USEPA, 2011). The calculation equations are described in the supplementary material S4. The reference dose (RfD) and slop factor (SF) applied in the risk characterization are given in Table S3.

Statistical analysis

The description statistical analysis of soil HM concentrations was conducted using SPSS 22.0 (IBM, Co, USA). Kolmogorov–Smirnov (K-S) test was used for normal test prior to the one-way analysis of variance. Logarithmic transformation should be used if the data don't meet the normal distribution. The spatial distribution maps were plotted by ordinary kriging interpolation using ArcGIS 10.2.2 (ESRI, Redlands, California, USA).

**Results and discussion**

HM concentrations in soils

The descriptive statistics of soil HMs in the study area are listed in Table 1. The K-S test showed that HM concentrations followed a normal distribution after a log-transformation ( $P > 0.05$ ) (Fig. S1), indicating that some soil samples were enriched with HMs. These statistical features suggest that geometric

**Table 1** Statistical summary of HMs in agricultural soils (mg/kg)

	Parameters	As	Cd	Cr	Cu	Ni	Pb	Zn
Entire study area	Min	12.30	1.06	13.28	43.54	27.34	26.28	128.05
	Max	85.88	9.77	252.12	124.86	120.52	181.12	2234.27
	Med	31.01	4.30	154.41	88.38	62.06	69.54	391.01
	AM	33.21	4.62	147.67	89.81	61.85	70.97	482.53
	SD	18.18	2.31	38.44	17.52	16.92	25.89	346.54
	GM	29.84	4.00	141.25	88.07	59.46	67.38	411.01
	CV(%)	54.74	50.00	26.03	19.51	27.36	36.48	71.81
	K-S test	0.00	0.00	0.00	0.01	0.02	0.01	0.00
Upstream area	Min	13.42	1.06	13.28	43.54	27.34	26.28	128.05
	Max	85.88	9.77	221.86	124.86	120.4	181.12	2234.27
	Med	35.78	4.49	129.49	86.46	62.83	73.35	439.56
	AM	39.07a	4.75a	138.09a	89.58a	60.90a	76.95a	563.53a
	SD	15.49	2.43	37.82	20.19	19.50	23.92	380.67
	GM	36.41	4.07	131.32	87.28	57.78	73.66	486.61
Downstream area	Min	12.30	1.29	112.12	79.00	51.05	29.50	144.15
	Max	45.50	8.63	211.12	122.01	90.04	110.00	454.45
	Med	17.50	4.15	125.65	89.01	62.06	50.60	265.68
	AM	19.22b	4.29a	137.59a	90.36a	64.09a	56.70b	289.17b
	SD	6.05	1.97	25.48	8.48	7.69	16.98	94.31
	GM	18.55	3.86	135.62	90.01	63.68	54.46	274.65
	BV	18.4	0.22	65.2	38.38	42.5	40.6	89.7
RSV	30	0.3	150	50	70	90	200	

*Min* minimum; *Max* maximum; *Med* median; *AM* arithmetic mean; *SD* standard deviation; *GM* geometric mean; *BV* background values; *RSV* risk screening values at pH 5.5 < pH ≤ 6.5

concentration was more representative of HM concentrations than arithmetic means. The concentrations of As, Pb, and Zn in the soils from the upstream area were significantly higher than those from downstream area ( $P < 0.05$ ). Cr (26.03%), Cu (19.51%), and Ni (27.36%) showed moderate spatial variation ( $15\% < CV < 36\%$ ) (Wilding, 1985), indicating a relatively homogeneous spatial distribution. In contrast, As (54.74%), Cd (50.00%), Pb (36.48%), and Zn (71.81%) exhibited high variation as the CV of these HMs exceeded 36% (Wilding, 1985). The high CV of HMs indicated greater spatial variability and the potential influence of anthropogenic activities.

The geo-mean concentrations of soil HMs were clearly higher than their corresponding background values in the Yunnan Province (CNEMC, 1990). In particular, geo-mean of Cd were 13.33 times the corresponding background value. When compared with the risk screening values (RSV) for China (MEPRC, 2018), As, Cd, Cr, Cu, Ni, Pb, and Zn in 51.43%, 100%, 35.24%, 97.14%, 29.53%, 16.19%, and 94.28% of soil samples exceeded their corresponding RSV values, respectively. These results indicate widespread HM pollution of agricultural soils in the study area.

Concentrations of HMs in this area were compared with data reported for other areas in foreign countries and China (Table S4). Concentrations of HMs in this study were higher than those in other foreign countries, although lower than those in floodplain agricultural soils along the Ibar River located in Southern Serbia and Northern Kosovo (Barać et al., 2016). The concentrations of As, Cd, Pb, and Zn were higher than those reported in soils from other areas in China, such as Gaogang (Cai et al., 2019), Jiedong (Jiang et al., 2020), and Hexi Corridor (Wang et al., 2020) (Table S4). The exception to this was Zhuzhou (Zhang et al., 2018) and Shaoguan (Xu et al., 2017), which are areas characterized by intensive mining and smelting activities.

#### Pollution characteristics of soil HMs

PI and PLI were used to assess the degree of HM pollution in the study area. The results indicated that Cd and Zn pollution levels were substantially higher than those of other HMs (Fig. S2a). In particular, Cd had the highest mean PI values among the HMs determined in the soils from the upstream (21.59)

and downstream areas (19.52); heavy pollution levels were observed in both areas. Moreover, multiple HMs in soils from upstream and downstream areas showed highly pollution levels, with mean PLI values of 3.07 and 2.45, respectively.

EF was applied to assess the influence of anthropogenic activities on HM enrichment in soils (Fig. S2b). Similar to PI values, the mean EF values were greater in the upstream areas than the downstream areas. EF values of all HMs were greater than 1, indicating anthropogenic influence. Cd exhibited very high enrichment in soils, with mean EF values of 24.94 and 22.55 in the soils from the upstream and downstream areas, respectively.

Overall, based on the PI, PLI, and EF, the soils in the study area were polluted with HMs to varying degrees and were heavily influenced by anthropogenic activities. As such, it was necessary to apportion the pollution sources of HMs in these agricultural soils.

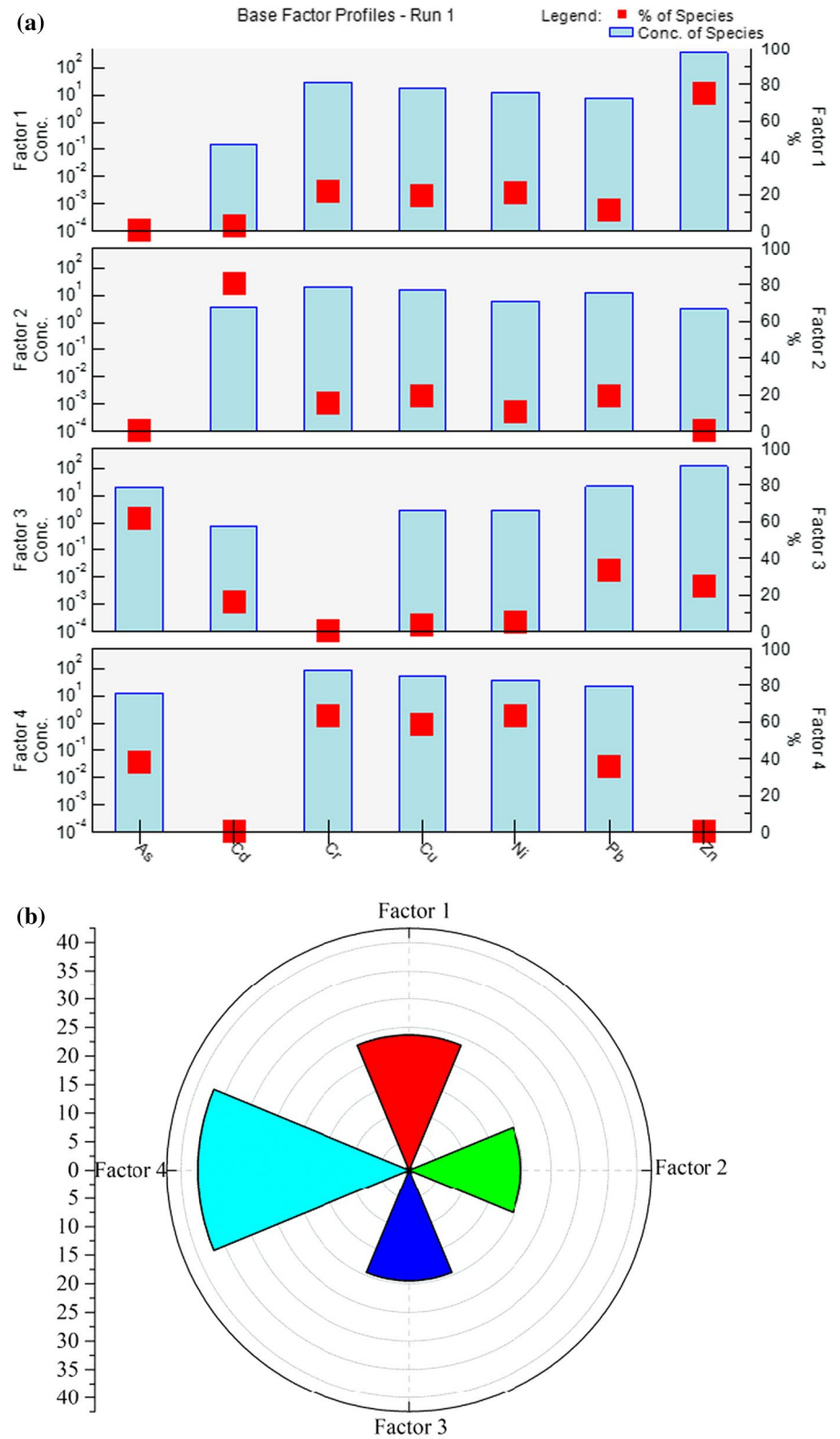
#### Source apportionment of soil HMs

##### *PMF model*

Two input files, including concentration data of seven HMs in 105 samples and their corresponding uncertainty data, are provided for PMF model. After examining the number of factors, four factors were determined based on the minimum and stable Q value. Meanwhile, the residuals of soil HMs were between  $-3$  and  $3$ . HMs with a signal-to-noise ratio ( $S/N$ )  $> 2$  were classified as strong, indicating rationality of the model (Table S1). The source profiles and source contributions of HMs in these soils are presented in Fig. 2.

The contribution of F1 to the investigated heavy metals decreased in the order of Zn (74.88%), Cr (21.65%), Ni (21.12%), Cu (19.29%), and Pb (11.76%) (Fig. 2a). The geo-mean concentration of Zn was 4.58 times the background value (Table 1). The pollution characteristics of HMs revealed that the agricultural soils were moderately enriched with Zn (Fig. S2b). Previous studies have reported that Zn in agricultural soils may originate from dry or wet precipitation of atmospheric particulates containing Zn around the Zn smelter (Xiao et al., 2019). According to the field investigation, there was Zn smelting and metal processing around the study area. It was reported 1058 kg of Zn was discharged into the

**Fig. 2** Source profile (a) and source contributions (b) of HMs in soils



environment (LPG, 2019). Moreover, the high normalized contributions of F1 were distributed around the Zn smelting industry (Fig. 3a). It may be concluded that Zn accumulation in agricultural soils was derived from smelting activities.

The second factor (F2) was mainly dominated by Cd with a loading value of 80.9%, followed by Pb (19.09%), Cu (18.95%), and Cr (14.94%) (Fig. 2a). It was noted that the geo-mean concentration of Cd was greater than the background value (Table 1). Previous studies have demonstrated that increased Cd concentrations in agricultural soils were strongly associated with the intensive utilization of phosphate fertilizers as Cd is usually present as an impurity in phosphate rocks (Atafar et al., 2010). Xiao et al. (2019) reported that Cd concentrations in superphosphate, ammonium dihydrogen phosphate, compound fertilizer, and organic fertilizer were 3.89, 3.55, 8.56, and 10.69 mg/kg. Based on the survey data from this study, approximately 300, 600, and 600 kg/hm<sup>2</sup> of superphosphate, compound fertilizers, and organic fertilizers were introduced into the soils each year to obtain high yields, respectively. The total Cd introduced into the soil was determined to be 1167, 5136, and 6,414 mg/hm<sup>2</sup> for superphosphate, compound fertilizers, and organic fertilizers, respectively. In addition, previous studies reported that the main source of Cd in agricultural soils was associated with industrial sewage application emitted from industrial process (Wu et al., 2020). Cd emission amount was up to 38.18 kg every year in the study area (LPG, 2019). Moreover, elevated normalized contributions of F2 were found in the south and middle part of the upstream area in this study (Fig. 3b). Therefore, Cd in soils was interpreted as a mixed source like long-time fertilizer and industrial sewage application. Similar results were observed in other field near the Pb–Zn mining areas in Guangdong (Xu et al., 2017), and industrial estate in Hunan (Zhang et al., 2018).

The third factor (F3) was characterized by As, with a loading value of 61.6%, followed by Pb (33.28%) and Zn (24.47%) (Fig. 2a). As shown in Table 1, the geo-mean concentration of As was greater than the background value. Inorganic As compounds, such as lead arsenate, sodium arsenate, and calcium arsenate, are the functional ingredients of pesticides or herbicides (Bhattacharya et al., 2007). Previous studies have reported that elevated As concentrations in agricultural soils are related to the long-term application

of As-based herbicides and pesticides (Li et al., 2016a, 2016b; Zhang et al., 2018). Wang et al. (2019) reported As concentrations in some herbicides ranged from 0.18 to 4.10 mg/kg, and the annual input of As from the application of herbicides was 0.28–3.84 mg/hm<sup>2</sup>. Therefore, F3 was regarded as the agrochemical utilization.

The decreasing loading values for Cr (63.4%), Cu (58.5%), Ni (63.6%), and Pb (35.9%) occurred for the fourth factor (F4) (Fig. 2a). A previous study showed that high Cr and Ni concentrations in the soils may be related to sewage irrigation (Liu et al., 2015) and parent materials (Cortada et al., 2018; Duan et al., 2020). However, HM concentrations in irrigation water in this area were much lower than the maximum allowable metal concentrations set by China (GB5084-2005, MEPRC, 2005) (Table S5), indicating Cr and Ni concentrations in the soils were not related with irrigation. However, high concentrations (Table 1) and moderate enrichment of Cr and Ni (Fig. S2b) in this study indicated the influence of anthropogenic activities. In reality, there are metal casting plants, cement plants, and construction material processing plants around the study area. This resulted in a large amount of smoke and dust containing Cr, Ni, Cu, and Pb emitted from these industries, which were ultimately deposited into the surrounding agricultural soils (Chen et al., 2016; Wang et al., 2020). The spatial distribution of the normalized contribution of F4 (Fig. 3d) indicated that there was a high contribution occurring downstream area downwind of these industrial plants. In addition, most studies have demonstrated that vehicle exhaust contributes to the accumulation of Pb in the soils; this may be due to the use of Pb as an antiknock agent in gasoline (Hjortenkrans et al., 2006). Although the phasing out of leaded gasoline has reduced the input of Pb in soils, recent studies have demonstrated that the slow wear of brakes and tires may emit Pb into the environment (Huang et al., 2015; Wang et al., 2019a, 2019b). Brake wear also contributed to the enrichment of Cu in soils via the deposition of dust containing Cu (Hjortenkrans et al., 2006; Li et al., 2016a, 2016b). In this study, there were the highway crossed the study area with high traffic volume and township roads around the study area. The township roads are the main pathway for industrial transportation, and the heavy traffic transporting ore and metallurgical products result in the Pb and Cu contamination. Therefore, atmospheric



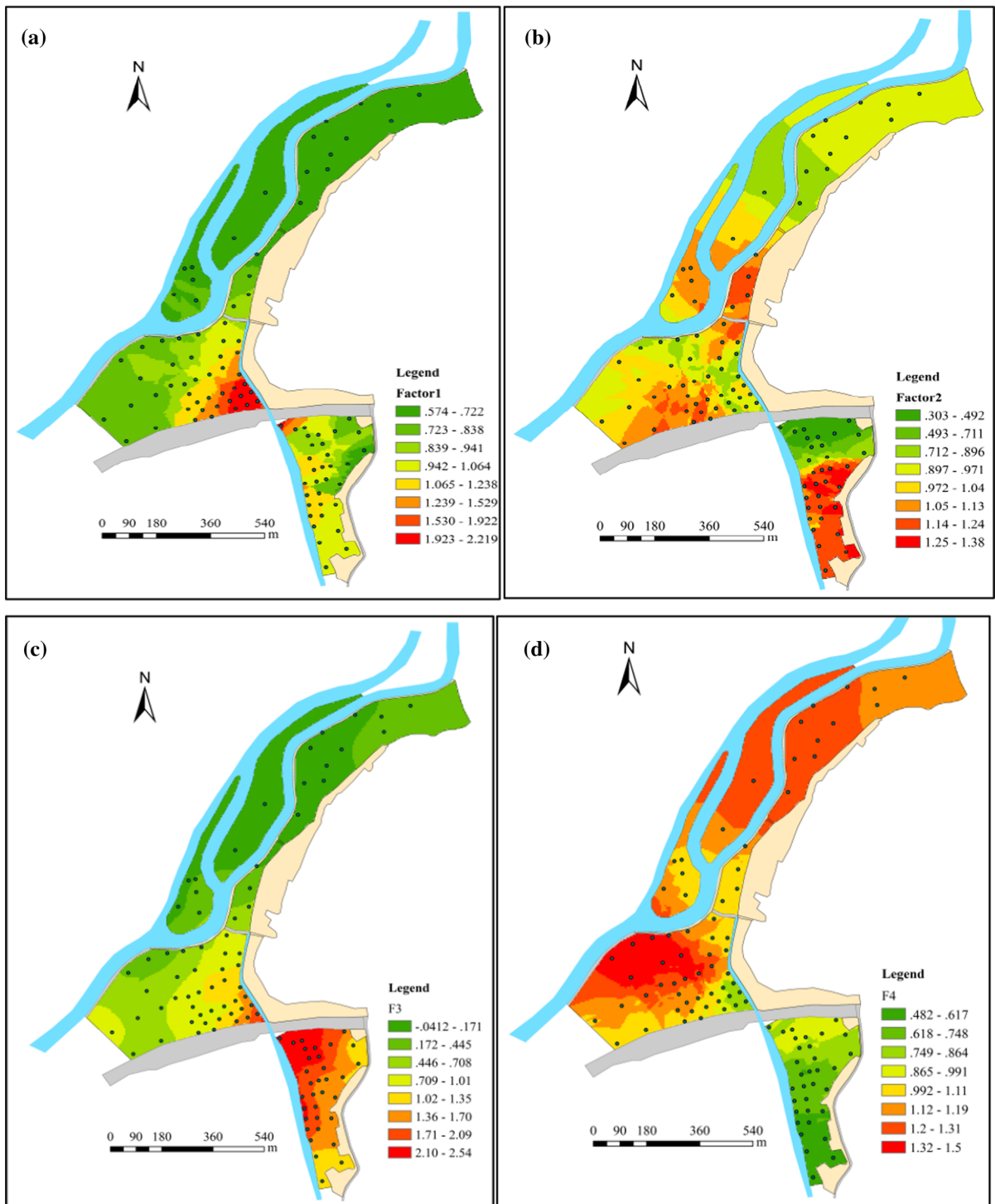


**Fig. 3** Distribution of normalized contributions of each factor in the study area (a) F1, (b) F2, (c) F3, (d) F4

deposition from industrial activities and traffic emissions may be responsible for the accumulation of Cr, Cu, Ni, and Pb in the soils; these findings are similar to the results reported by Zhang et al. (2018) in Zhuzhou, and Li et al. (2020) in Shanghai. Therefore, F4 may be regarded as atmospheric deposition from industrial and traffic emissions.

The proportion of each factor to the concentrations of HM was calculated (Fig. 2b), based on the source contribution of individual HMs. Among these sources, atmospheric deposition had the highest contribution to HM accumulation in soils, contributing a 37.11% proportion. Smelting activities contributed to 23.69% of the HMs in the soils; this was the second largest contribution. The mixed source including fertilizer and industrial sewage application accounted for 19.69% proportion. However, the agricultural input cannot be ignored despite it being the lowest contributor in terms of HM accumulation in the soils, with the proportions 19.51%.

#### *Uncertainty analysis*

The coefficients of determination ( $R^2$ ) for the measured and predicted concentrations were greater than 0.50 for all HMs (Table S1, Fig. S3). This indicates that PMF model fitting adequately explains the information included in the concentrations of HMs (Huang et al., 2018). It was noted that the  $R^2$  of Pb was only 0.515 and Fig. S3 shows that the predicted Pb concentrations fitted the measured concentrations well at most sites except for site 74. The measured Pb concentrations at site 74 (outlier) were significantly higher compared with Pb concentrations at other sites, which may be associated with the specific event or site accounted for the outlier (Pan et al., 2018). Previous studies have demonstrated that outliers in the data may affect the distribution of HM concentrations and further influence the PMF model results (Yang et al., 2019; Zhi et al., 2016). Therefore, the uncertainty of PMF results should be further analyzed.

BS and DISP methods were conducted based on the different algorithms to verify the reliability and robustness of the PMF model. For BS analysis, it is used to identify whether there are a small set of observations that can disproportionately influence the PMF results. For each BS run, the factors derived from PMF were mapped to those of the base run. In this study, each factor of BS run was assigned to the

base factors ( $R^2 > 0.6$ ), and the mapping of BS factors to base factors was 94%, 100%, 94%, and 99% for F1, F2, F3, and F4, respectively, indicating the results of PMF were reliable. For DISP analysis, it is used to understand the selected solution in finer detail, including its sensitivity to small changes (rotational ambiguity), and the DISP swaps is an important indicator of the stability of the results of PMF. In this study, the decrease in dQ (DISP % dQ) was lower than 1% (Table S6), and DISP swaps was not occurred at the  $Q(dQ_{\max})$  level, which indicated that four factors selected in this study were reasonable and the results were stable (USEPA, 2014).

Additionally, the variability in contributions to soil HMs derived from BS is displayed in Fig. S4. Some uncertainties existed in the contributions of source factors derived from PMF model. For example, the base run value of Cd in factor 4 was higher than 75th percentile values derived from BS, which can be attributed to that the random errors influence the contribution of base run. The great variation of Cd concentrations in soils (Table 1) explained larger random error of Cd distribution among the soil samples. Moreover, the interval ratios based on the BS and DISP for each factor are shown in Fig. S5. The interval ratios of Cd in F1, As and Cd in F4 were slightly higher than 2, indicating uncertainties exist for these factors. However, HMs with high loading in each factor, such as Zn in F1, Cd in F2, As in F3, and Cr, Cu, Ni, and Pb in F4, have lower uncertainties as the interval ratios of these heavy metals were substantial lower than 2, indicating little rotational ambiguity and random error. Overall, these results suggest that the uncertainties can be interpreted and the results may be appropriate (USEPA, 2014).

#### *Source-specific health risk apportionment*

For the non-carcinogenic risk, HI and THI values of HMs for adults from four sources were less than the safe value of 1 (Fig. 4a, Table S7), whereas THI values for children from four sources were greater than 1 (Fig. 4b, Table S7). THI values for adults and children in this study were lower than those from the agricultural soils in Wenling (11.8 for children and 6.73 for adults) where a cluster of e-waste dismantling workshops accommodated (Yang et al., 2019). However, they were higher than those from the sewage irrigation areas in Tianjin (Female: 0.13,

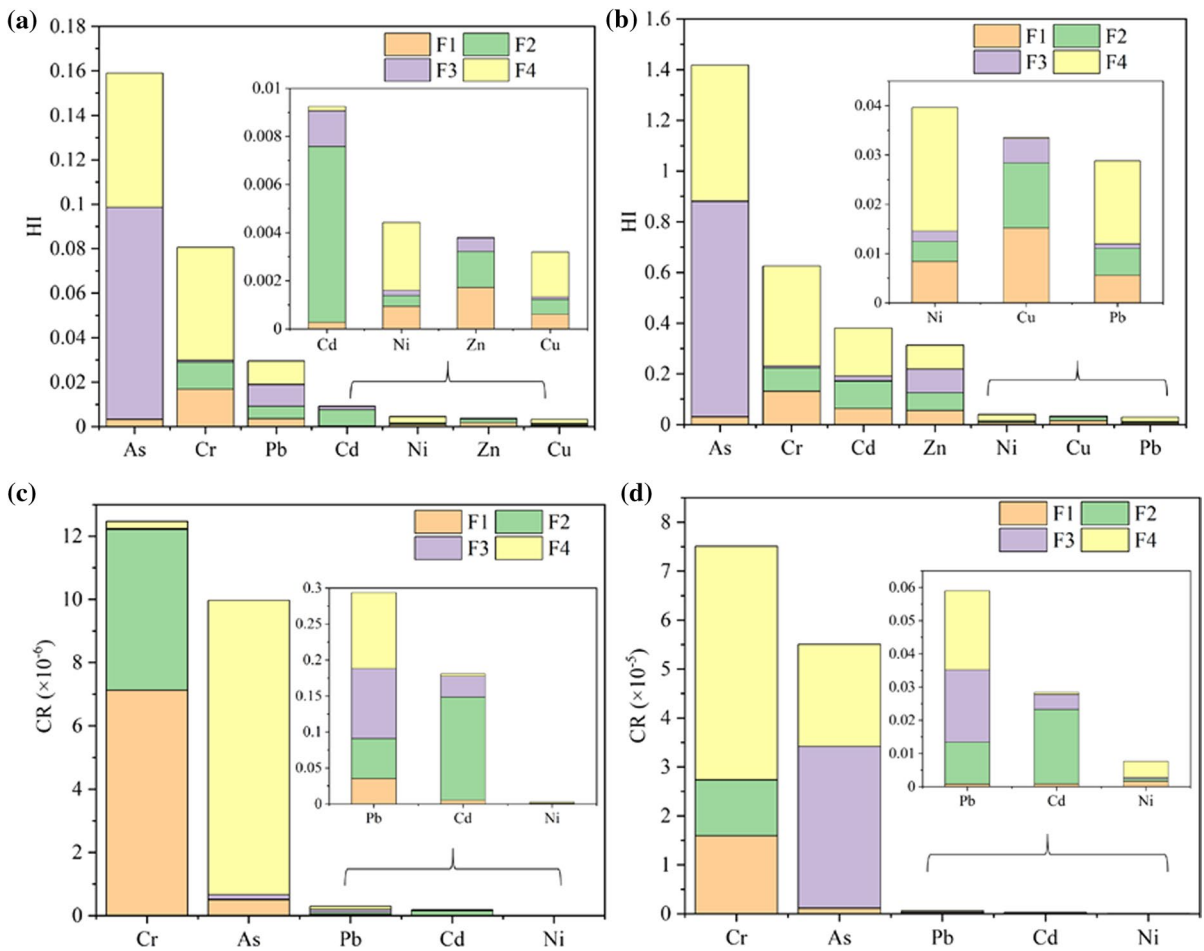


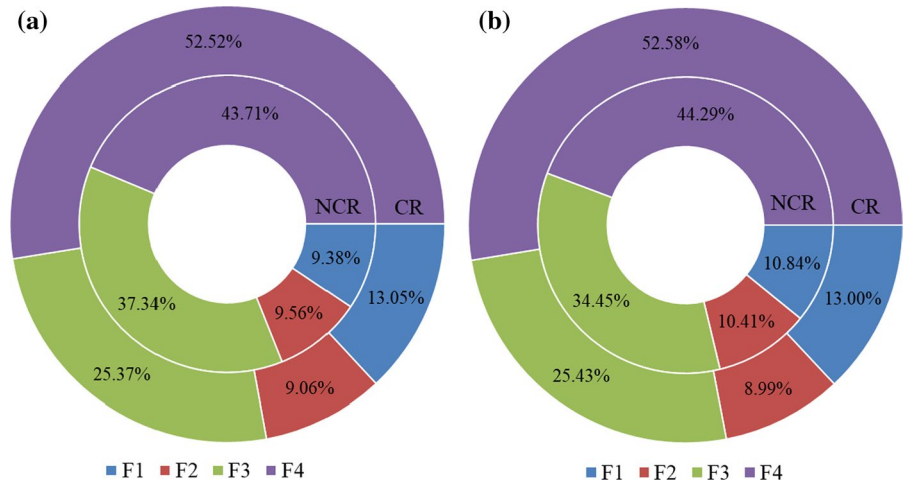
**Fig. 4** Non-carcinogenic and carcinogenic risks of individual HMs from four sources for adults (a, c) and children (b, d)

Male: 0.08, children: 0.41) (Wu et al., 2020). For carcinogenic risk, the risk to adults was acceptable as the TCR values were within  $1 \times 10^{-6}$  and  $1 \times 10^{-4}$  (Fig. 4c, Table S7), while the potential carcinogenic risk for children cannot be ignored as the TCR values were slightly greater than  $1 \times 10^{-4}$  (Table S7). These results highlight that the non-carcinogenic and carcinogenic risks were greater for children than adults; this is consistent with other studies that showed children had the highest health risks (Jiang et al., 2021; Yang et al., 2019). This may be associated with the higher respiration rate per unit body weight and gastrointestinal absorption of HMs for children, and the pica and hand sucking behavior they generally exhibit (Wei et al., 2015).

Similar trends in the contribution proportion from potential four sources were found for adults (Fig. 5a)

and children (Fig. 5b). As shown in Fig. 5a, atmospheric deposition (F4) had the highest contribution to non-carcinogenic and carcinogenic risks for adults, with contributions of 43.71% and 52.52%, respectively. This may be attributed to this source being predominantly loaded by Cr, Ni, Pb, and Cu (Fig. 2a) with higher toxicity. Other studies have also reported high adverse carcinogenic effects posed by Cr and Ni (Cao et al., 2016; Murari et al., 2020) due to their high SFs and lower RfD values (USEPA, 2011). In contrast, mixed source from fertilizer application and waste disposal (F2) contributed the lowest to non-carcinogenic and carcinogenic risks, with contribution proportions of 9.56% and 9.06% for adults (Fig. 5a), and 8.99% and 10.41% for children (Fig. 5b), respectively.

**Fig. 5** The proportional contribution to human health risks from four sources for (a) adults; and (b) children



To further understand the health risk and associated with contributions of different sources, we compared the results of this study with the similar researches studied in China (Table S8). As seen in Table S8, the contributions of sources to the health risk were similar between adults and children, which confirmed the results of this study. However, agricultural activities contributed most to the non-carcinogenic risk for both adults and children in previous studies (Huang et al., 2018; Jiang et al., 2020; Wang et al., 2020; Yang et al., 2019) but they were second contributors to non-carcinogenic and carcinogenic risks. Similarly, industrial activities contributed the most the carcinogenic risk. Overall, the different contribution of each source may be attributed to the toxicity or bioavailability of the HMs in the soils.

It was noted that source contributions to human risk (Fig. 5) were different from contribution to the accumulation of HMs in soils (Fig. 2b). For example, the contribution proportion of agrochemical utilization to the accumulation of HMs was the lowest, but its non-carcinogenic and carcinogenic risks to adults had increased by 17.85% and 5.86%, respectively. This may be because agrochemical activities in this study were dominated by As with relatively low RfD and high SF values. Similar results were reported by Yang et al. (2019), who reported that the highest contribution to THI values for adults and children was from agrochemical application. In contrast, the non-carcinogenic and carcinogenic risks to adults from smelting activities was 14.31% and 10.64% lower, respectively,

compared to its contribution to the accumulation of HMs in the soils; this may be due to the lower toxicity of Zn (IRIS, 2003).

#### Spatial distributions of source-specific health risks

A similar spatial distribution of non-carcinogenic and carcinogenic risks was observed for adults (Fig. 6) and children (Fig. S6). As such, only the distribution of health risks for adults has been discussed here.

The similar distribution trends were observed for contribution of F1 to non-carcinogenic risk (Fig. 6a) and carcinogenic risk (Fig. 6e). As seen in Fig. 5, health risk distribution presented a decreased trend from upstream to downstream. In addition, the distribution of the contribution of F3 to human health risk (Fig. 6c and g) was similar to that of normalized contribution of F3 (Fig. 3c). This may be because As was the dominant element for both F3 and human health risks. However, the distribution of contribution of F1 to health risk was slightly different with the spatial distribution of normalized contribution of F1 (Fig. 3a). Similarly, there were clear differences between the spatial distributions of the normalized contribution of F4 (Fig. 3c) and the contribution of F4 to human health risk (Fig. 6d and h). Overall, priority zones were recognized based on source-specific risks and located at the upstream area. Therefore, source-specific health risk results suggest that greater attention is required for the priority zones.

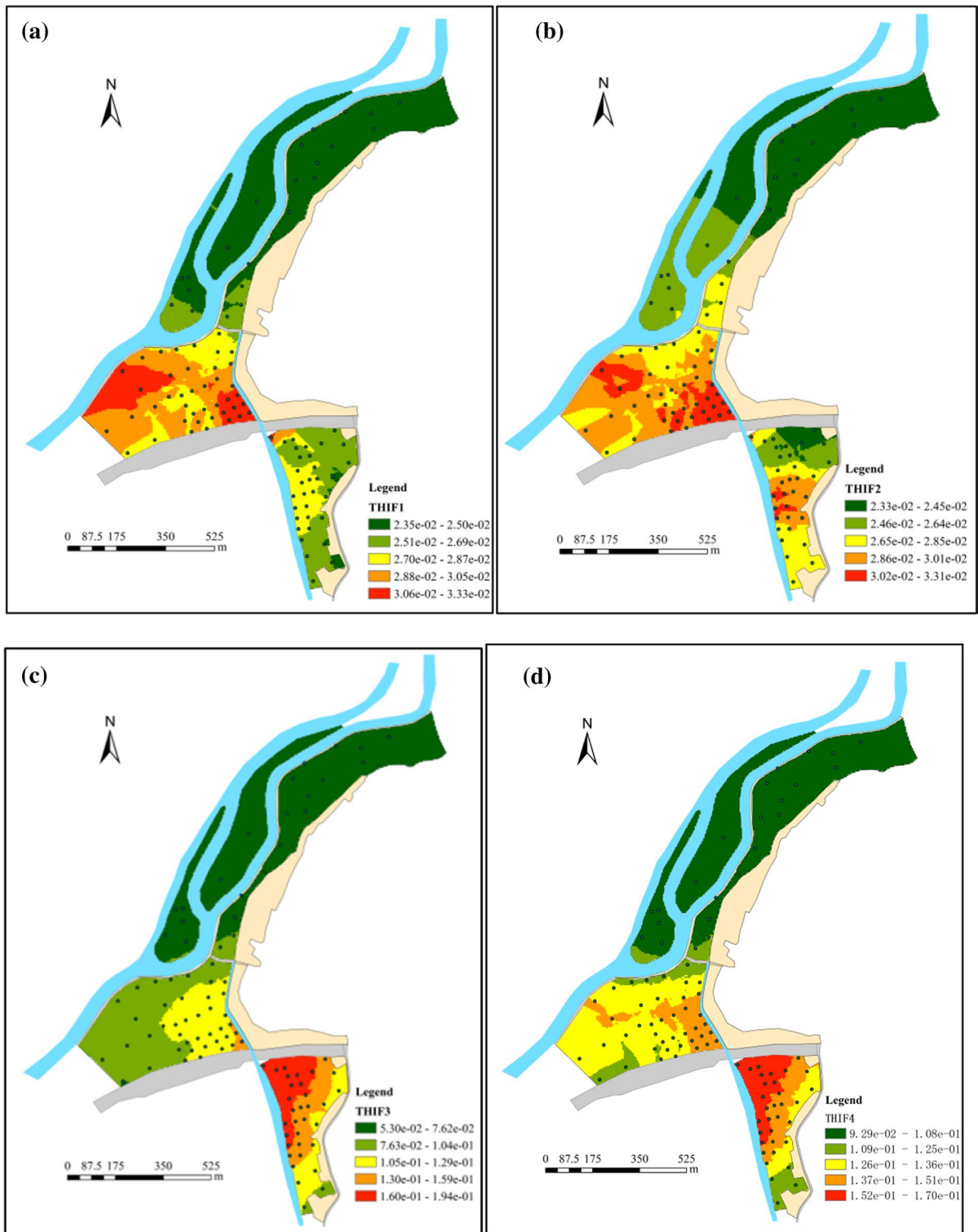


**Fig. 6** Spatial distribution of source contribution to non-carcinogenic (a–d) and carcinogenic risks (e–h) for adults

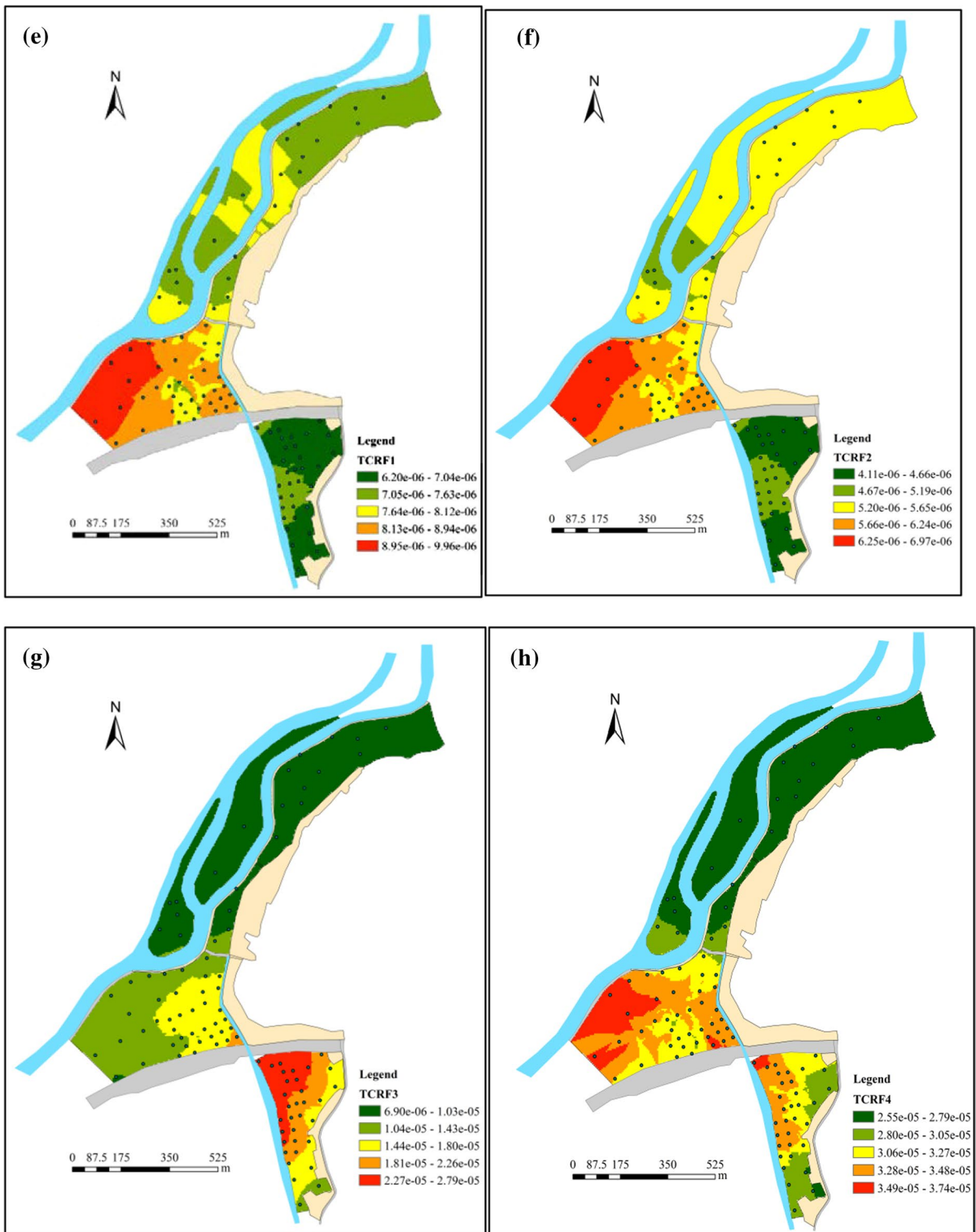


Fig. 6 (continued)

## Conclusions and future prospects

In this study, pollution levels and source apportionment of soil HMs were explored. The geo-mean concentrations of As, Cd, Cu, Cr, Ni, Pb, and Zn exceeded their corresponding background values. The PLI and EF values of HMs indicated that the soils were highly polluted with HMs, particularly Cd. Four potential sources, including smelting activities, fertilizer and industrial sewage application, agrochemical utilization, and atmospheric deposition, were identified and apportioned using the PMF model, with contributions of 37.11%, 23.69%, 19.69%, and 19.51%, respectively. In addition, an approach combining the risk assessment with PMF model was used to quantitatively characterize the source-specific health risk apportionment from four potential sources. The result highlighted that atmospheric deposition caused the highest health risks to both children and adults. Priority zones were identified at upstream area based on the distribution of source-specific human health risks.

Overall, this study provides an effective approach to quantify source-specific health risks for human, which is vital for pollution prevent and risk controlling for soil HMs. In despite of it, PMF model should be improved due to its sensitivity to the outlier of the dataset. The future researches combining the emission inventory, migration transformation model, and epidemiological investigation with PMF are needed to improve the accurate of the source-specific risk apportionment result for soil HMs.

**Author contributions** GG: Writing-Original draft preparation, Software, Investigation. YW: Data curation, Conceptualization, Methodology. DZ: Writing-Reviewing and Editing. KL: Writing-Reviewing and Editing. ML: Validation, Visualization, Investigation.

**Funding** This work was supported by the National Key Research and Development Program of China [grant number 2018YFC1800104].

**Data availability** We make sure that all data and materials as well as software application support our published claims and comply with field standards.

## Declarations

**Conflict of interest** The authors declare that they have no known competing financial interests or personal relationships that could have appeared to influence the work reported in this paper.

**Ethical approval** We assured that this study did not involve any ethical experiments.

**Consent for publication** Depending on the ownership of the journal and its policies, we will grant the Publisher an exclusive license to publish the article or transfer copyright of the article to the Publisher.

## References

- Atafar, Z., Mesdaghinia, A., Nouri, J., Homaei, M., Yunesian, M., Ahmadi Moghaddam, M., & Mahvi, A. H. (2010). Effect of fertilizer application on soil heavy metal concentration. *Environmental Monitoring and Assessment*, *160*, 83–89. <https://doi.org/10.1007/s10661-008-0659-x>
- Barać, N., Škrivanj, S., Bukumirić, Z., Živojinović, D., Manojlović, D., Barać, M., Petrović, R., & Ćorac, A. (2016). Distribution and mobility of heavy elements in floodplain agricultural soils along the Ibar River (Southern Serbia and Northern Kosovo). Chemometric investigation of pollutant sources and ecological risk assessment. *Environmental Science and Pollution Research*, *23*, 9000–9011. <https://doi.org/10.1007/s11356-016-6142-2>
- Bhattacharya, P., Welch, A. H., Stollenwerk, K. G., McLaughlin, M. J., Bundschuh, J., & Panullah, G. (2007). Arsenic in the environment: Biology and Chemistry. *Science of the Total Environment*, *379*, 109–120. <https://doi.org/10.1016/j.scitotenv.2007.02.037>
- Cai, L. M., Wang, Q. S., Wen, H. H., Luo, J., & Wang, S. (2019). Heavy metals in agricultural soils from a typical township in Guangdong Province, China: Occurrences and spatial distribution. *Ecotoxicology and Environmental Safety*, *168*, 184–191. <https://doi.org/10.1016/j.ecoenv.2018.10.092>
- Cao, S., Duan, X., Zhao, X., Chen, Y., Wang, B., Sun, C., Zheng, B., & Wei, F. (2016). Health risks of children's cumulative and aggregate exposure to metals and metalloids in a typical urban environment in China. *Chemosphere*, *147*, 404–411. <https://doi.org/10.1016/j.chemosphere.2015.12.134>
- Chen, H., Teng, Y., Chen, R., Li, J., & Wang, J. (2016). Contamination characteristics and source apportionment of trace metals in soils around Miyun Reservoir. *Environmental Science and Pollution Research*, *23*, 15331–15342. <https://doi.org/10.1007/s11356-016-6694-1>
- CNEMC (China National Environmental Monitor Center), 1990. The soil background values in China. Environmental Science Press, Beijing (in Chinese).
- Cortada, U., Hidalgo, M. C., Martínez, J., & Rey, J. (2018). Impact in soils caused by metal(loid)s in lead metallurgy. The case of La Cruz Smelter (Southern Spain). *Journal of Geochemical Exploration*, *190*, 302–313. <https://doi.org/10.1016/j.gexplo.2018.04.001>
- Duan, X. C., Yu, H. H., Ye, T. R., Huang, Y., Li, J., Yuan, G. L., & Albanese, S. (2020). Geostatistical mapping and quantitative source apportionment of potentially toxic elements in top- and sub-soils: A case of suburban area

- in Beijing, China. *Ecological Indicators*, 112, 106085. <https://doi.org/10.1016/j.ecolind.2020.106085>
- Guo, G. H., Wang, Y. T., Zhang, D. G., & Lei, M. (2021). Source-specific ecological and health risks of potential toxic elements in agricultural soils in Southern Yunnan Province and associated uncertainty analysis. *Journal of Hazardous Materials*, 417, 126144.
- Hjortenkrans, D., Bergbäck, B., & Häggerud, A. (2006). New metal emission patterns in road traffic environments. *Environmental Monitoring and Assessment*, 117, 85–98. <https://doi.org/10.1007/s10661-006-7706-2>
- Hu, J., Lin, B., Yuan, M., Lao, Z., Wu, K., Zeng, Y., Liang, Z., Li, H., Li, Y., Zhu, D., Liu, J., & Fan, H. (2019). Trace metal pollution and ecological risk assessment in agricultural soil in Dexing Pb/Zn mining area, China. *Environmental Geochemistry and Health*, 41, 967–980. <https://doi.org/10.1007/s10653-018-0193-x>
- Huang, Y., Li, T., Wu, C., He, Z., Japenga, J., Deng, M., & Yang, X. (2015). An integrated approach to assess heavy metal source apportionment in peri-urban agricultural soils. *Journal of Hazardous Materials*, 299, 540–549. <https://doi.org/10.1016/j.jhazmat.2015.07.041>
- Huang, J., Guo, S., Zeng, G. M., Li, F., Gu, Y., Shi, Y., Shi, L., Liu, W., & Peng, S. (2018). A new exploration of health risk assessment quantification from sources of soil heavy metals under different land use. *Environmental Pollution*, 243, 49–58. <https://doi.org/10.1016/j.envpol.2018.08.038>
- Jiang, H. H., Cai, L. M., Wen, H. H., Hu, G. C., Chen, L. G., & Luo, J. (2020). An integrated approach to quantifying ecological and human health risks from different sources of soil heavy metals. *Science of the Total Environment*. <https://doi.org/10.1016/j.scitotenv.2019.134466>
- Jiang, H. H., Cai, L. M., Hu, G. C., Wen, H. H., Luo, J., Xu, H. Q., & Chen, L. G. (2021). An integrated exploration on health risk assessment quantification of potentially hazardous elements in soils from the perspective of sources. *Ecotoxicology and Environmental Safety*, 208, 111489. <https://doi.org/10.1016/j.ecoenv.2020.111489>
- Khademi, H., Gabarrón, M., Abbaspour, A., Martínez-Martínez, S., Faz, A., & Acosta, J. A. (2019). Environmental impact assessment of industrial activities on heavy metals distribution in street dust and soil. *Chemosphere*, 217, 695–705. <https://doi.org/10.1016/j.chemosphere.2018.11.045>
- Khadhar, S., Sdiri, A., Chekirben, A., Azouzi, R., & Charef, A. (2020). Integration of sequential extraction, chemical analysis and statistical tools for the availability risk assessment of heavy metals in sludge amended soils. *Environmental Pollution*, 263, 114543. <https://doi.org/10.1016/j.envpol.2020.114543>
- Li, Y., Ye, F., Wang, A., Wang, D., Yang, B., Zheng, Q., Sun, G., & Gao, X. (2016a). Chronic arsenic poisoning probably caused by arsenic-based pesticides: Findings from an investigation study of a household. *International Journal of Environmental Research and Public Health*. <https://doi.org/10.3390/ijerph13010133>
- Li, S. Q., Zhang, G. L., Yang, J. L., & Jia, N. (2016b). Multi-source characteristics of atmospheric deposition in Nanjing, China, as controlled by East Asia monsoons and urban activities. *Pedosphere*, 26, 374–385. [https://doi.org/10.1016/S1002-0160\(15\)60050-9](https://doi.org/10.1016/S1002-0160(15)60050-9)
- Li, Y., Yuan, Y., Sun, C., Sun, T., Liu, X., Li, J., Fang, L., & Fan, Z. (2020). Heavy metals in soil of an urban industrial zone in a metropolis: Risk assessment and source apportionment. *Stochastic Environmental Research and Risk Assessment*, 34, 435–446. <https://doi.org/10.1007/s00477-020-01779-z>
- Liu, Y., Wang, H., Li, X., & Li, J. (2015). Heavy metal contamination of agricultural soils in Taiyuan, China. *Pedosphere*, 25, 901–909. [https://doi.org/10.1016/S1002-0160\(15\)30070-9](https://doi.org/10.1016/S1002-0160(15)30070-9)
- Liu, J., Liu, Y. J., Liu, Y., Liu, Z., & Zhang, A. N. (2018). Quantitative contributions of the major sources of heavy metals in soils to ecosystem and human health risks: A case study of Yulin, China. *Ecotoxicology and Environmental Safety*, 164, 261–269. <https://doi.org/10.1016/j.ecoenv.2018.08.030>
- Luoping People' Government (LPG). 2019. Luoping year-book. Luoping People's Publishing House. 65
- Marrugo-Negrete, J., Pinedo-Hernández, J., & Díez, S. (2017). Assessment of heavy metal pollution, spatial distribution and origin in agricultural soils along the Sinú River Basin, Colombia. *Environmental Research*, 154, 380–388. <https://doi.org/10.1016/j.envres.2017.01.021>
- MEPRC (Ministry of Environmental Protection of the People's Republic of China), 2002. Technical specifications requirements for monitoring of surface water and waste water. HJ/T 91-2002, (In Chinese).
- MEPRC (Ministry of Environmental Protection of the People's Republic of China), 2005. Standards for irrigation water quality (GB 5084–2005) (in Chinese).
- MEPRC (Ministry of Environmental Protection of the People's Republic of China), 2018. Soil environmental quality risk control standard for soil contamination of agricultural land (GB 15618-2018) (in Chinese).
- Murari, V., Singh, N., Ranjan, R., Singh, R. S., & Banerjee, T. (2020). Source apportionment and health risk assessment of airborne particulates over central Indo-Gangetic Plain. *Chemosphere*, 257, 127145. <https://doi.org/10.1016/j.chemosphere.2020.127145>
- Pan, Z., Liu, P., Gao, S., Feng, M., & Zhang, Y. (2018). Evaluation of flood season segmentation using seasonal exceedance probability measurement after outlier identification in the three gorges reservoir. *Stochastic Environmental Research and Risk Assessment*, 32, 1573–1586. <https://doi.org/10.1007/s00477-018-1522-4>
- Standardization administration of People's Public of China (SAPRC). (2019). Classification and codes for Chinese soil (GB GB/T17296-2009. (in Chinese)
- USEPA (United States Environment Protection Agency). 1989. Risk Assessment Guidance for Superfund Vol. I: Human Health Evaluation Manual. EPA/540/1-89/002. Office of Solid Waste and Emergency Response. Washington, DC.
- USEPA (United States Environment Protection Agency). 2014. EPA positive matrix factorization (PMF) 5.0 fundamentals and user guide. Washington, DC.
- USEPA (United States Environmental Protection Agency), 2011. Exposure Factors Handbook. (final ed.), EPA/600/R-09/052F., Washington, DC.
- USEPA, 1996. Acid digestion of sediment, sludge, and soils. Method 3050B. Revision 2, Washington DC



- Wang, L., Gao, S., Yin, X., Yu, X., & Luan, L. (2019a). Arsenic accumulation, distribution and source analysis of rice in a typical growing area in north China. *Ecotoxicology and Environmental Safety*, *167*, 429–434. <https://doi.org/10.1016/j.ecoenv.2018.10.015>
- Wang, S., Cai, L. M., Wen, H. H., Luo, J., Wang, Q. S., & Liu, X. (2019b). Spatial distribution and source apportionment of heavy metals in soil from a typical county-level city of Guangdong Province, China. *Science of the Total Environment*, *655*, 92–101. <https://doi.org/10.1016/j.scitotenv.2018.11.244>
- Wang, F., Guan, Q., Tian, J., Lin, J., Yang, Y., Yang, L., & Pan, N. (2020). Contamination characteristics, source apportionment, and health risk assessment of heavy metals in agricultural soil in the Hexi Corridor. *CATENA*, *191*, 104573. <https://doi.org/10.1016/j.catena.2020.104573>
- Wei, X., Gao, B., Wang, P., Zhou, H., & Lu, J. (2015). Pollution characteristics and health risk assessment of heavy metals in street dusts from different functional areas in Beijing, China. *Ecotoxicology and Environmental Safety*, *112*, 186–192. <https://doi.org/10.1016/j.ecoenv.2014.11.005>
- Wilding, L. P. (1985). Spatial variability: Its documentation, accommodation, and implication to soil surveys. In D. R. Nielsen & J. Bouma (Eds.), *Soil spatial variability* (pp. 166–194). Wageningen, The Netherlands: Pudoc.
- Wu, J., Li, J., Teng, Y., Chen, H., & Wang, Y. (2020). A partition computing-based positive matrix factorization (PC-PMF) approach for the source apportionment of agricultural soil heavy metal contents and associated health risks. *Journal of Hazardous Materials*, *388*, 121766. <https://doi.org/10.1016/j.jhazmat.2019.121766>
- Xiao, R., Guo, D., Ali, A., Mi, S., Liu, T., Ren, C., Li, R., & Zhang, Z. (2019). Accumulation, ecological-health risks assessment, and source apportionment of heavy metals in paddy soils: A case study in Hanzhong, Shaanxi, China. *Environmental Pollution*, *248*, 349–357. <https://doi.org/10.1016/j.envpol.2019.02.045>
- Xu, D. M., Yan, B., Chen, T., Lei, C., Lin, H. Z., & Xiao, X. M. (2017). Contaminant characteristics and environmental risk assessment of heavy metals in the paddy soils from lead (Pb)-zinc (Zn) mining areas in Guangdong Province, South China. *Environmental Science and Pollution Research*, *24*, 24387–24399. <https://doi.org/10.1007/s11356-017-0052-9>
- Yang, S., He, M., Zhi, Y., Chang, S. X., Gu, B., Liu, X., & Xu, J. (2019). An integrated analysis on source-exposure risk of heavy metals in agricultural soils near intense electronic waste recycling activities. *Environment International*. <https://doi.org/10.1016/j.envint.2019.105239>
- Zhang, X., Wei, S., Sun, Q., Wadood, S. A., & Guo, B. (2018). Source identification and spatial distribution of arsenic and heavy metals in agricultural soil around Hunan industrial estate by positive matrix factorization model, principle components analysis and geo statistical analysis. *Ecotoxicology and Environmental Safety*, *159*, 354–362. <https://doi.org/10.1016/j.ecoenv.2018.04.072>
- Zheng, H., Kong, S., Yan, Q., Wu, F., Cheng, Y., Zheng, S., Wu, J., Yang, G., Zheng, M., Tang, L., Yin, Y., Chen, K., Zhao, T., Liu, D., Li, S., Qi, S., Zhao, D., Zhang, T., Ruan, J., & Huang, M. (2019). The impacts of pollution control measures on PM<sub>2.5</sub> reduction: Insights of chemical composition, source variation and health risk. *Atmospheric Environment*, *197*, 103–117. <https://doi.org/10.1016/j.atmosenv.2018.10.023>
- Zhi, Y., Li, P., Shi, J., Zeng, L., & Wu, L. (2016). Source identification and apportionment of soil cadmium in cropland of Eastern China: A combined approach of models and geographic information system. *Journal of Soils and Sediments*, *16*, 467–475. <https://doi.org/10.1007/s11368-015-1263-7>

**Publisher's Note** Springer Nature remains neutral with regard to jurisdictional claims in published maps and institutional affiliations.